ELSEVIER

Engineering Analysis with Boundary Elements 31 (2007) 667–682

ENGINEERING ANALYSIS with BOUNDARY ELEMENTS

www.elsevier.com/locate/enganabound

An alternating iterative algorithm for the Cauchy problem in anisotropic elasticity

Lucia Comino[a], Liviu Marin[b,*], Rafael Gallego[a]

[a]*Department of Structural Mechanics, University of Granada, 18071 Granada, Spain*
[b]*School of Mechanical, Materials and Manufacturing Engineering, The University of Nottingham, Nottingham NG7 2RD, UK*

Received 2 October 2006; accepted 18 December 2006
Available online 6 March 2007

Abstract

The alternating iterative algorithm proposed by Kozlov et al. [An iterative method for solving the Cauchy problem for elliptic equations. USSR Comput Math Math Phys 1991;31:45–52] for obtaining approximate solutions to the Cauchy problem in two-dimensional anisotropic elasticity is analysed and numerically implemented using the boundary element method (BEM). The ill-posedness of this inverse boundary value problem is overcome by employing an efficient regularising stopping. The numerical results confirm that the iterative BEM produces a convergent and stable numerical solution with respect to increasing the number of boundary elements and decreasing the amount of noise added into the input data.

Keywords: Boundary element method (BEM); Anisotropic elasticity; Cauchy problem; Inverse problem; Regularisation

1. Introduction

In solving physical problems in solid mechanics, one usually deals with the governing system of partial differential equations, i.e. the equilibrium equations, which has to be solved provided that the geometry of the domain of interest, the material properties, the external sources acting in the solution domain and the boundary and initial conditions are completely known. These are referred to as *direct problems* and their well-posedness has been clearly established, see for example Knops and Payne [1]. When one or more of the conditions for solving the direct problem are partially or entirely unknown then an *inverse problem* may be formulated to determine the unknowns from specified or measured system responses. It is well known that inverse problems are in general unstable, see e.g. Hadamard [2], in the sense that small measurement errors in the input data may amplify significantly the errors in the solution. Hence a suitable algorithm, which is exempted from this ill-posed phenomenon, is required in order to stably solve the inverse problem.

Over the last two decades, inverse problems have been extensively treated in several branches of science, such as heat transfer [3], electrical impedance tomography [4], acoustic and electromagnetic scattering [5] and solid mechanics [6], etc. The most common approach is to determine the optimal estimates of the model parameters by minimising a measure-to-fit between the responses of the system and the model. The mathematical mechanism which shows that Cauchy problems are ill-posed has been explained by Chen and Chen [7] for the Laplace equation. Similarly, the Cauchy problem in elasticity, in which both the displacement and the traction vectors are known on a part of the boundary and no data are available on the remaining boundary, is a classical example of an inverse problem in solid mechanics.

There are important studies in the literature of the Cauchy problem for isotropic elastic materials. Maniatty et al. [8] have determined the traction boundary conditions by using a simple diagonal regularisation in conjunction with the finite element method (FEM). Spatial regularisation, together with the boundary element method (BEM),

*Corresponding author. Tel.: +44 115 846 7683; fax: +44 115 951 3800.
E-mail address: liviu.marin@nottingham.ac.uk (L. Marin).

0955-7997/$ - see front matter © 2007 Elsevier Ltd. All rights reserved.
doi:10.1016/j.enganabound.2006.12.009

has been used by Zabaras et al. [9] and with the FEM by Schnur and Zabaras [10]. Yeih et al. [11] have analysed the existence, uniqueness and continuous dependence on the data of the Cauchy problem in elasticity and have proposed an alternative regularisation procedure, namely the fictitious boundary indirect method, based on the simple or double layer potential theory. The numerical implementation of the aforementioned method has been undertaken by Koya et al. [12], who have used the BEM and the Nyström method for discretising the integrals. However, this formulation has not yet removed the problem of multiple integrations. Marin et al. [13] have determined the approximate solutions to the Cauchy problem in linear elasticity using an alternating iterative BEM which reduced the problem to solving a sequence of well-posed mixed boundary value problems and they have later extended this numerical method to singular Cauchy problems, see Marin et al. [14]. Huang and Shih [15] and Marin et al. [16] have both used the conjugate gradient method (CGM) combined with the BEM, in order to solve the same problem. The Tikhonov regularisation method and the singular value decomposition (SVD), in conjunction with the BEM, have been employed by Marin and Lesnic [17,18] to solve the two-dimensional Cauchy problem in isotropic linear elasticity. A comparison of the aforementioned BEM regularisation methods, namely the alternating iterative algorithm, CGM, SVD and the Tikhonov regularisation method, used for solving the Cauchy problem for isotropic linear elastic solids can be found in Marin et al. [19]. Recently, the method of fundamental solutions combined with the first-order Tikhonov functional and the Landweber method in conjunction with the BEM and a regularising stopping criterion have been proposed by Marin and Lesnic [20,21], respectively.

Methods of obtaining an approximate solution to ill-posed boundary value problems have been discussed extensively in the literature, see e.g. Lavrent'ev [22], Tikhonov and Arsenin [23], Bakushinsky and Goncharsky [24], Morozov [25], etc., and at present there are various approaches to the solution of the Cauchy problem for elliptic equations, which is a classical example of an ill-posed problem. On the whole, all such approaches can be divided into three large groups. The first group consists of methods based on bringing the problem into the class of well-posedness in the sense of Tikhonov, see e.g. Lavrent'ev [22]. The second group comprises methods that use universal regularising algorithms, which can be obtained with the aid of the Tikhonov parametric functional, or related versions of it, see e.g. Tikhonov and Arsenin [23]. Unfortunately, this last group requires a parametric selection which may prove to be difficult in real circumstances. Finally, the most recently developed group includes iterative direct solution methods, see e.g. Bakushinsky and Goncharsky [24]. These have produced the main results and are the most widely used in practical applications. Of all these groups, the latter one has two main advantages, namely (i) it allows any physical constraint, e.g. positivity, monotonicity, etc., to be easily taken into account directly in the scheme of the iterative algorithm, and (ii) it allows simplicity of the implementation of the computational schemes to be used iteratively for a sequence of well-posed problems. One possible disadvantage of using iterative algorithms is the large number of iterations that may be required in order to achieve convergence. However, relaxation procedures can be easily adopted to improve the rate of convergence.

Based on these reasons, we have decided in this study to use the BEM in order to implement a convergent algorithm for anisotropic linear elastic materials based on an alternating iterative procedure which consists of obtaining successive solutions to well-posed mixed boundary value problems. This numerical method was originally proposed by Kozlov et al. [26] and implemented for isotropic linear elastic solids by Marin et al. [13,14]. The strength of this iterative algorithm is that it is convergent if and only if the solution of the Cauchy problem exists, which overcomes the previous mathematical redundancy. Whilst Kozlov et al. [26] proved the mathematical convergence of their algorithm without actually finding the solution, the aim of this paper is to show the numerical stability and convergence of the present algorithm as it determines an approximation of the solution to the Cauchy problem in anisotropic elasticity. In order to cease the iterative procedure before the effects of the accumulation of noise become dominant and the errors in the numerical solution start increasing, a regularising stopping criterion is proposed.

2. Mathematical formulation of the Cauchy problem in two-dimensional anisotropic linear elasticity

Consider an anisotropic linear elastic homogeneous solid which occupies an open bounded domain $\Omega \subset \mathbb{R}^2$ and assume that Ω is bounded by a smooth surface Γ in the sense of Liapunov, such that $\Gamma = \Gamma_1 \cup \Gamma_2$, where $\Gamma_1, \Gamma_2 \neq \emptyset$ and $\Gamma_1 \cap \Gamma_2 = \emptyset$. In particular, we consider the case when the geometry and the loading conditions describe a pure plane strain state. Therefore, the problem variables, i.e. displacements, stresses and strains, can be simplified to a two-dimensional study.

In the presence of body forces $\mathbf{b}$, the equilibrium equations of the elastic medium are given by, see e.g. Lekhnitskii [27],

$$\operatorname{div}(\boldsymbol{\sigma}(\mathbf{u})) + \mathbf{b} = \mathbf{0} \quad \text{in } \Omega, \tag{1}$$

where $\boldsymbol{\sigma}$ is the stress tensor. On assuming small deformations only, the strain tensor $\boldsymbol{\varepsilon} = (\nabla \mathbf{u} + \nabla^{\mathrm{T}} \mathbf{u})/2$ is related to the stress tensor $\boldsymbol{\sigma}$ by Hooke's constitutive law, namely

$$\boldsymbol{\sigma} = \mathbf{C} : \boldsymbol{\varepsilon} \quad \text{in } \Omega, \tag{2}$$

where $\mathbf{C}$ is the elasticity tensor of order four. The traction vector $\mathbf{t}$ at a point on the boundary Γ with the outward

normal $\mathbf{n}$ is defined by

$$\mathbf{t} = \boldsymbol{\sigma} \cdot \mathbf{n} \quad \text{on } \Gamma. \tag{3}$$

The constitutive law (2) for two-dimensional anisotropic linear elastic solids is usually expressed using a mono-index notation[1]

$$\sigma_i = c_{ij}\varepsilon_j, \quad \varepsilon_i = a_{ij}\sigma_j, \quad i,j = 1,\ldots,6, \tag{4}$$

where ε_j is the strain tensor, c_{ij} is the elasticity tensor and a_{ij} is the compliance tensor.

If it is possible to measure both the displacement and traction vectors on a part of the boundary Γ, say $\Gamma_2 \subset \Gamma$, and there is no information on the remaining boundary $\Gamma_1 = \Gamma/\Gamma_2$ then this leads to the mathematical formulation of an inverse problem consisting of the equilibrium equation (1) (for simplicity, in the absence of body forces, i.e. $\mathbf{b} = 0$) and the given over-specified boundary conditions on Γ_2, namely

$$\begin{cases} \operatorname{div}(\boldsymbol{\sigma}(\mathbf{u})) = 0 & \text{in } \Omega, \\ \mathbf{u} = \widetilde{\mathbf{u}} & \text{on } \Gamma_2, \\ \mathbf{t} = \widetilde{\mathbf{t}} & \text{on } \Gamma_2. \end{cases} \tag{5}$$

Here $\widetilde{\mathbf{u}}$ and $\widetilde{\mathbf{t}}$ are prescribed vector valued displacements and tractions, respectively. In the above formulation of the boundary conditions (5_2) and (5_3), it can be seen that the boundary Γ_2 is over-specified by prescribing both the displacement $\mathbf{u}|_{\Gamma_2} = \widetilde{\mathbf{u}}$ and the traction $\mathbf{t}|_{\Gamma_2} = \widetilde{\mathbf{t}}$ vectors, whilst the boundary Γ_1 is under-specified since both the displacement $\mathbf{u}|_{\Gamma_1}$ and the traction $\mathbf{t}|_{\Gamma_1}$ vectors are unknown and have to be determined. This problem, termed the *Cauchy problem*, is much more difficult to solve both analytically and numerically than the direct problem, since the solution does not satisfy the general conditions of well-posedness. Although the problem may have a unique solution, it is well known that this solution is unstable with respect to small perturbations in the data on Γ_2, see Hadamard [2]. Thus the problem is ill-posed and we cannot use a direct approach, such as the Gauss elimination method, in order to solve the system of linear equations which arises from the discretisation of the partial differential equation and the boundary conditions (5).

3. Description of the algorithm

Knowing the exact data $\widetilde{\mathbf{u}}$ and $\widetilde{\mathbf{t}}$ on the boundary Γ_2, we use a convergent iterative algorithm, originally proposed by Kozlov et al. [26] and implemented for isotropic linear elastic media by Marin et al. [13,14], but with a regularising stopping criterion which is essential when the data $\widetilde{\mathbf{u}}$ and/or $\widetilde{\mathbf{t}}$ become noisy. This algorithm consists of the following steps:

Step 1.1: Set $k = 0$. Specify an initial approximation $\boldsymbol{t}^{(0)}$ for the tractions on the under-specified boundary Γ_1.

[1] $11 \to 1$, $22 \to 2$, $33 \to 3$, $23 \to 4$, $13 \to 5$, $12 \to 6$.

Step 1.2: Solve the mixed boundary value problem

$$\begin{cases} \operatorname{div}(\boldsymbol{\sigma}(\boldsymbol{u}^{(1)})) = 0 & \text{in } \Omega, \\ \boldsymbol{t}^{(1)} \equiv \boldsymbol{\sigma}(\boldsymbol{u}^{(1)}) \cdot \boldsymbol{n} = \boldsymbol{t}^{(0)} & \text{on } \Gamma_1, \\ \boldsymbol{u}^{(1)} = \widetilde{\boldsymbol{u}} & \text{on } \Gamma_2 \end{cases} \tag{6}$$

in order to determine the displacements $\boldsymbol{u}^{(1)}$ in Ω and on Γ_1.

Step 2.1: Having constructed the approximation $\boldsymbol{u}^{(2k-1)}$, $k>0$, the mixed boundary value problem

$$\begin{cases} \operatorname{div}(\boldsymbol{\sigma}(\boldsymbol{u}^{(2k)})) = 0 & \text{in } \Omega, \\ \boldsymbol{u}^{(2k)} = \boldsymbol{u}^{(2k-1)} & \text{on } \Gamma_1, \\ \boldsymbol{t}^{(2k)} \equiv \boldsymbol{\sigma}(\boldsymbol{u}^{(2k)}) \cdot \boldsymbol{n} = \widetilde{\boldsymbol{t}} & \text{on } \Gamma_2 \end{cases} \tag{7}$$

is solved to determine the displacements $\boldsymbol{u}^{(2k)}$ in Ω and the tractions $\boldsymbol{t}^{(2k)} \equiv \boldsymbol{\sigma}(\boldsymbol{u}^{(2k)}) \cdot \boldsymbol{n}$ on Γ_1.

Step 2.2: Having constructed the tractions $\boldsymbol{t}^{(2k)}$, $k>0$, the mixed boundary value problem

$$\begin{cases} \operatorname{div}(\boldsymbol{\sigma}(\boldsymbol{u}^{(2k+1)})) = 0 & \text{in } \Omega, \\ \boldsymbol{t}^{(2k+1)} \equiv \boldsymbol{\sigma}(\boldsymbol{u}^{(2k+1)}) \cdot \boldsymbol{n} = \boldsymbol{t}^{(2k)} & \text{on } \Gamma_1, \\ \boldsymbol{u}^{(2k+1)} = \widetilde{\boldsymbol{u}} & \text{on } \Gamma_2 \end{cases} \tag{8}$$

is solved in order to determine the displacements $\boldsymbol{u}^{(2k+1)}$ in Ω and on Γ_1.

Step 3: Set $k = k + 1$ and repeat steps 2.1 and 2.2 until a prescribed stopping criterion is satisfied.

Let $H^1(\Omega)$ be the Sobolev space and $H^{1/2}(\Gamma) \times H^{1/2}(\Gamma)$ be the space of traces on Γ corresponding to $H^1(\Omega) \times H^1(\Omega)$, see e.g. Lions and Magenes [28]. We denote by $H^{1/2}(\Gamma_i) \times H^{1/2}(\Gamma_i)$ the space of functions from $H^{1/2}(\Gamma) \times H^{1/2}(\Gamma)$ that are bounded on Γ_i and by $(H^{1/2}(\Gamma_i) \times H^{1/2}(\Gamma_i))^*$ the dual space of $H^{1/2}(\Gamma_i) \times H^{1/2}(\Gamma_i)$ for $i = 1, 2$. Kozlov et al. [26] showed that if Γ is smooth, $\widetilde{\boldsymbol{u}} \in H^{1/2}(\Gamma_2) \times H^{1/2}(\Gamma_2)$ and $\widetilde{\boldsymbol{t}} \in (H^{1/2}(\Gamma_2) \times H^{1/2}(\Gamma_2))^*$, then the alternating algorithm based on steps 1–3 produces two sequences of approximate solutions $\{\boldsymbol{u}^{(2k)}(\boldsymbol{x})\}_{k>0}$ and $\{\boldsymbol{u}^{(2k-1)}(\boldsymbol{x})\}_{k>0}$ which both converge in $H^1(\Omega) \times H^1(\Omega)$ to the solution $\boldsymbol{u}(\boldsymbol{x})$ of the Cauchy problem (5) for any initial guess $\boldsymbol{t}^{(0)} \in (H^{1/2}(\Gamma_1) \times H^{1/2}(\Gamma_1))^*$. Moreover, the alternating algorithm has a regularising character. Also the same conclusion is obtained if at the step 1.1 we specify an initial guess $\boldsymbol{u}^{(0)} \in H^{1/2}(\Gamma_1) \times H^{1/2}(\Gamma_1)$, instead of an initial guess for the traction vector $\boldsymbol{t}^{(0)} \in (H^{1/2}(\Gamma_1) \times H^{1/2}(\Gamma_1))^*$, and we modify accordingly the steps 1 and 2 of the algorithm.

We note that if the initial guess $\boldsymbol{t}^{(0)}$ is in $(H^{1/2}(\Gamma_1) \times H^{1/2}(\Gamma_1))^*$ and the boundary data $\widetilde{\boldsymbol{u}}$ and $\widetilde{\boldsymbol{t}}$ are in $H^{1/2}(\Gamma_2) \times H^{1/2}(\Gamma_2)$ and $(H^{1/2}(\Gamma_2) \times H^{1/2}(\Gamma_2))^*$, respectively, the problems (6)–(8) are well-posed and solvable in $H^1(\Omega) \times H^1(\Omega)$, see Lions and Magenes [28]. These intermediate mixed well-posed problems are solved using the BEM described in the next section. In order to pass from one iteration to the next, the values of the displacement and traction vectors are required only on the boundary Γ and not in the domain Ω and, therefore, the BEM is a very suitable technique for solving the intermediate mixed boundary value problems (6)–(8).

Furthermore, the displacements and stresses inside the solution domain Ω have to be evaluated only after the stopping criterion has been satisfied and not at every iteration, thus saving a substantial amount of computational time and storage requirements.

4. The boundary element method

The BEM is based on the boundary integral representation of the displacements. This technique is derived from Betti's Reciprocity Theorem applied to the actual elastostatic state in the domain Ω and an auxiliary field called the fundamental solution.

4.1. Fundamental solution

The fundamental solution is the response of a system at a point $\mathbf{z}$ due to a point load applied at $\mathbf{z}'$ in an infinite domain with the same material properties as the original problem. Based on complex potential theory, the anisotropic displacement U_{ij} and stress T_{ij} fundamental solutions are given by, see e.g. Lekhnitskii [27] and Sollero [29],

$$U_{ij}(\mathbf{z},\mathbf{z}') = 2\,\mathrm{Re}[p_{j1}A_{i1}\ln(z_1 - z_1') + p_{j2}A_{i2}\ln(z_2 - z_2')], \quad (9)$$

$$T_{ij}(\mathbf{z},\mathbf{z}') = 2\,\mathrm{Re}\left[\frac{q_{j1}A_{i1}}{z_1 - z_1'}(\mu_1 n_1 - n_2) + \frac{q_{j2}A_{i2}}{z_2 - z_2'}(\mu_2 n_1 - n_2)\right]. \quad (10)$$

Here $z_i = x_1 + \mu_i x_2$, x_1 and x_2 are the two-dimensional Cartesian coordinates, n_i are the components of the outward normal to the boundary Γ and μ_i are two conjugate pairs, roots of the characteristic fourth degree polynomial equation

$$\beta_{11}\mu^4 - 2\beta_{16}\mu^3 + (\beta_{12} + \beta_{66})\mu^2 - 2\beta_{16}\mu + \beta_{22} = 0, \quad (11)$$

where β_{ij} are the so-called reduced elastic constants whose values are given by $\beta_{ij} = a_{ij}$ for the plane stress state and $\beta_{ij} = a_{ij} - (a_{i3}a_{j3})/a_{33}$ for the plane strain state. Furthermore, $q_{1i} = \mu_i$, $q_{2i} = -1$, p_{ik} are given by

$$p_{1k} = \beta_{11}\mu_k^2 + \beta_{12} - \beta_{16}\mu_k,$$
$$p_{2k} = \beta_{12}\mu_k + \frac{\beta_{22}}{\mu_k} - \beta_{26}, \quad k = 1,2, \quad (12)$$

whilst the complex constants A_{ij} are obtained from the implementation of the boundary conditions, i.e. they are computed by solving the following system of equations

$$\begin{pmatrix} 1 & -1 & 1 & -1 \\ \mu_1 & -\bar{\mu}_1 & \mu_2 & -\bar{\mu}_2 \\ p_{11} & -\bar{p}_{11} & p_{12} & -\bar{p}_{12} \\ p_{21} & -\bar{p}_{21} & p_{22} & -\bar{p}_{22} \end{pmatrix} \begin{pmatrix} A_{i1} \\ \bar{A}_{i1} \\ A_{i2} \\ \bar{A}_{i2} \end{pmatrix} = \begin{pmatrix} \frac{\delta_{i2}}{2\pi\imath} \\ \frac{\delta_{i1}}{2\pi\imath} \\ 0 \\ 0 \end{pmatrix}, \quad (13)$$

where $\imath^2 = -1$ and δ_{ij} is the Kronecker delta tensor.

4.2. Boundary integral equation (BIE)

Once the auxiliary state is defined, we recall Betti's Reciprocity Theorem which is applied to two balanced systems of boundary and body forces $(\mathbf{t},\mathbf{b})$ and $(\mathbf{t}^*,\mathbf{b}^*)$. These systems of forces are applied to the same anisotropic elastic domain characterised by the displacement fields $\mathbf{u}$ and $\mathbf{u}^*$, respectively. If the $*$ state is the one given by the fundamental solution, namely

$$b_j^* = \delta_{ij}\delta(\mathbf{z} - \mathbf{z}'), \quad t_j^* = T_{ij}(\mathbf{z},\mathbf{z}'), \quad u_j^* = U_{ij}(\mathbf{z},\mathbf{z}'), \quad (14)$$

where $\mathbf{z}'$ is a point inside the solution domain Ω, on assuming that no body forces act on the solid, i.e. $\mathbf{b} = 0$ in (1), then Somigliana identity is obtained as

$$u_i(\mathbf{z}') + \int_\Gamma T_{ij}(\mathbf{z},\mathbf{z}')u_j(\mathbf{z})\,\mathrm{d}\Gamma = \int_\Gamma U_{ij}(\mathbf{z},\mathbf{z}')t_j(\mathbf{z})\,\mathrm{d}\Gamma. \quad (15)$$

By moving $\mathbf{z}'$ to the limit at a boundary point $\mathbf{y} \in \Gamma$, i.e. $\mathbf{z}' \to \mathbf{y}$, we obtain the BIE which governs the elastic displacement field and is given by

$$c_{ij}(\mathbf{y})u_j(\mathbf{y}) + \int_\Gamma T_{ij}(\mathbf{z},\mathbf{y})u_j(\mathbf{z})\,\mathrm{d}\Gamma = \int_\Gamma U_{ij}(\mathbf{z},\mathbf{y})t_j(\mathbf{z})\,\mathrm{d}\Gamma, \quad (16)$$

where the free term $c_{ij}(\mathbf{y})$ depends on the location of the collocation point $\mathbf{z}'$, see e.g. Brebbia and Dominguez [30] and París and Cañas [31].

4.3. Discretisation of the BIE (16)

In order to solve numerically the BIE (16), the boundaries Γ, Γ_1 and Γ_2 are discretised into N_e, N_e^1 and N_e^2 elements, respectively, such that $N_e^1 + N_e^2 = N_e$. The geometry, displacements and stresses are interpolated over each element using their values at the nodes and some shape functions ϕ_m. For every collocation point l with the coordinates $\mathbf{y}^l$ the BIE (16) can be written in discretised form as

$$c_{ij}u_j(l) + \sum_{k=1}^{N_e}\sum_{m=1}^{3} h_{ij}^m(l,k)u_j^k(m) = \sum_{k=1}^{N_e}\sum_{m=1}^{3} g_{ij}^m(l,k)t_j^k(m), \quad (17)$$

where the integration constants $h_{ij}^m(l,k)$ and $g_{ij}^m(l,k)$, $i,j = 1,2$, $m = 1,2,3$, are given by

$$h_{ij}^m(l,k) = \int_{-1}^{1} T_{ij}(\mathbf{z}(\xi),\mathbf{y}^l)\phi_m(\xi)J^k(\xi)\,\mathrm{d}\xi, \quad (18)$$

$$g_{ij}^m(l,k) = \int_{-1}^{1} U_{ij}(\mathbf{z}(\xi),\mathbf{y}^l)\phi_m(\xi)J^k(\xi)\,\mathrm{d}\xi, \quad (19)$$

whilst $J^k(\xi)$ is the Jacobian of the transformation of the boundary element Γ_k into the interval $[-1,1]$ in the parametric space.

In this study, isoparametric quadratic elements have been used such that if the boundary Γ is closed and is discretised into N_e elements then the total number of boundary nodes is given by $N = 2N_e$. Consequently, the number of boundary nodes corresponding to the

under-specified Γ_1 and over-specified Γ_2 boundaries is given by $N_1 = 2N_e^1$ and $N_2 = 2N_e^2$, respectively, such that $N_1 + N_2 = N$. The values of the integration constants are detailed in the Appendix.

On collocating Eq. (17) at all the boundary nodes, we obtain the following system of linear algebraic equations:

$$\mathbf{HU} = \mathbf{GT}, \tag{20}$$

where $\mathbf{U}$ and $\mathbf{T}$ are vectors containing the nodal values of the displacements and tractions, respectively. The discretisation of the boundary conditions (5_2) and (5_3) provides the values of $4N_2$ of the unknowns and the problem reduces to solving a system of $2N$ equations with $4N_1$ unknowns which can be generically written as

$$\mathbf{CX} = \mathbf{F}, \tag{21}$$

where the matrix $\mathbf{C} \in \mathbb{R}^{2N\times 4N_1}$ depends solely on the geometry of the boundary and the material properties, the vector $\mathbf{X} \in \mathbb{R}^{4N_1}$ contains the unknown values of the displacements and the tractions on the boundary Γ_1 and the vector $\mathbf{F} \in \mathbb{R}^{2N}$ is computed using the Cauchy boundary conditions (5_2) and (5_3).

5. Numerical results

In this section we illustrate the numerical results obtained using the iterative algorithm presented in Section 3, in conjunction with the BEM described in Section 4. In addition, we investigate the convergence with respect to the mesh size discretisation and the number of iterations when the data are exact, and the stability when the data are perturbed by noise.

5.1. Examples

In order to present the performance of the numerical method proposed, we solve the Cauchy problem for three examples associated with an orthotropic linear elastic medium (birch plywood), whose material orthotropy axes coincide with the axes of the Cartesian reference system. The orthotropic solid considered in this study is characterised by the engineering elastic constants $E_1 = 11.76\,\mathrm{GN/m^2}$, $E_2 = 5.88\,\mathrm{GN/m^2}$, $G_{12} = 0.686\,\mathrm{GN/m^2}$ and $\nu_{12} = 0.071$ and hence the compliance elastic constants are given by $a_{11} = 0.08503\,\mathrm{m^2/GN}$, $a_{12} = -0.006037\,\mathrm{m^2/GN}$, $a_{22} = 0.1701\,\mathrm{m^2/GN}$, $a_{66} = 1.4577\,\mathrm{m^2/GN}$ and $a_{16} = a_{26} = 0.0\,\mathrm{m^2/GN}$.

Example 1. We consider a stress state corresponding to constant internal and external pressures $\sigma_i = 1.0\,\mathrm{GN/m^2}$ and $\sigma_e = 2.0\,\mathrm{GN/m^2}$, respectively, in the annular domain $\Omega = \{\mathbf{x} = (x_1, x_2) | r_i^2 < x_1^2 + x_2^2 < r_o^2\}$, $r_i = 1$, $r_o = 4$, see Fig. 1(a). The under- and over-specified boundaries are given by $\Gamma_1 = \Gamma_i \equiv \{\mathbf{x} \in \Gamma | x_1^2 + x_2^2 = r_i^2\}$ and $\Gamma_2 = \Gamma_o \equiv \{\mathbf{x} \in \Gamma | x_1^2 + x_2^2 = r_0^2\}$, respectively.

Example 2. We consider a uniform hydrostatic stress state given by $\sigma_e = \sigma_i = 1.5\,\mathrm{GN/m^2}$ in the annular domain $\Omega = \{\mathbf{x} = (x_1, x_2) | r_i^2 < x_1^2 + x_2^2 < r_0^2\}$, $r_i = 1$, $r_0 = 4$, see Fig. 1(b). Here the under- and over-specified boundaries are given by $\Gamma_1 = \{\mathbf{x} \in \Gamma_i | \alpha_1 \leqslant \Theta(\mathbf{x}) \leqslant \alpha_2\}$ and $\Gamma_2 = \Gamma_0 \cup \{\mathbf{x} \in \Gamma_i | 0 \leqslant \Theta(\mathbf{x}) < \alpha_1\} \cup \{\mathbf{x} \in \Gamma_i | \alpha_2 < \Theta(\mathbf{x}) \leqslant 2\pi\}$, respectively, where $\Theta(\boldsymbol{x})$ is the angular polar coordinate of $\boldsymbol{x}$ and α_i, $i = 1, 2$, are specified angles in the interval $(0, 2\pi)$. In order to illustrate the typical numerical results, we have taken $\alpha_1 = \pi/4$ and $\alpha_2 = 3\pi/4$.

Example 3. We consider the unit square plate with an elliptical traction-free cavity, whose half-axes are given by $a = 0.2$ and $b = 0.1$, subject to a plane stress state corresponding to the loading conditions shown in Fig. 1(c). Here the under- and over-specified boundaries are given by the inner (cavity) and the outer boundaries of the plate, respectively.

Although analytical expressions for the stresses $\boldsymbol{\sigma}^{(\mathrm{an})}$ can be obtained and hence analytical expressions for the traction vector $\mathbf{t}^{(\mathrm{an})}$, it should be noted that the corresponding analytical displacements $\mathbf{u}^{(\mathrm{an})}$ are not available in this case, but they can be obtained numerically by solving the direct problem

$$\begin{cases} \mathrm{div}(\boldsymbol{\sigma}^{(\mathrm{an})}(\mathbf{u}^{(\mathrm{an})})) = 0 & \text{in } \Omega, \\ \boldsymbol{\sigma}^{(\mathrm{an})}(\mathbf{u}^{(\mathrm{an})}) \cdot \mathbf{n} = \mathbf{t}^{(\mathrm{an})} & \text{on } \Gamma, \end{cases} \tag{22}$$

where the rigid body displacements are eliminated by using

$$\int_\Omega \mathbf{u}^{(\mathrm{an})}\,\mathrm{d}\Omega = 0 \quad \text{and} \quad \int_\Omega \mathbf{u}^{(\mathrm{an})} \times \mathbf{x}\,\mathrm{d}\Omega = 0. \tag{23}$$

Hence the Cauchy problem considered in this paper is described by Eq. (5), in which the Cauchy data are given $\widetilde{\mathbf{t}} = \mathbf{t}^{(\mathrm{an})}$ and $\widetilde{\mathbf{u}} = \mathbf{u}^{(\mathrm{an})}$, where the displacement vector $\mathbf{u}^{(\mathrm{an})}$ is obtained by solving numerically the Neumann problem (22), together with the rigid body conditions (23), with a very fine BEM mesh in order to obtain its best numerical approximation. In the sequel, the analytical traction vector $\mathbf{t}^{(\mathrm{an})}$ and the corresponding displacement vector $\mathbf{u}^{(\mathrm{an})}$ will be referred to as "exact" traction and displacement vectors, respectively.

The Cauchy problems given by Eq. (5) for the examples considered in this study have been solved iteratively using the BEM to provide simultaneously the unspecified boundary displacement and traction vectors on the boundary Γ_2. The number of isoparametric quadratic boundary elements used for discretising the boundary Γ in Examples 1 and 2 was taken to be $N_e \in \{32, 48, 96\}$ such that both the under- and over-specified boundaries Γ_1 and Γ_2, respectively, were discretised into the same number of isoparametric quadratic boundary elements, namely $N_e/2 \in \{16, 24, 48\}$. In the case of Example 3, the boundaries Γ_1 and Γ_2 were discretised into 20 and 24 isoparametric quadratic elements, respectively, such that $N_e = 44$.

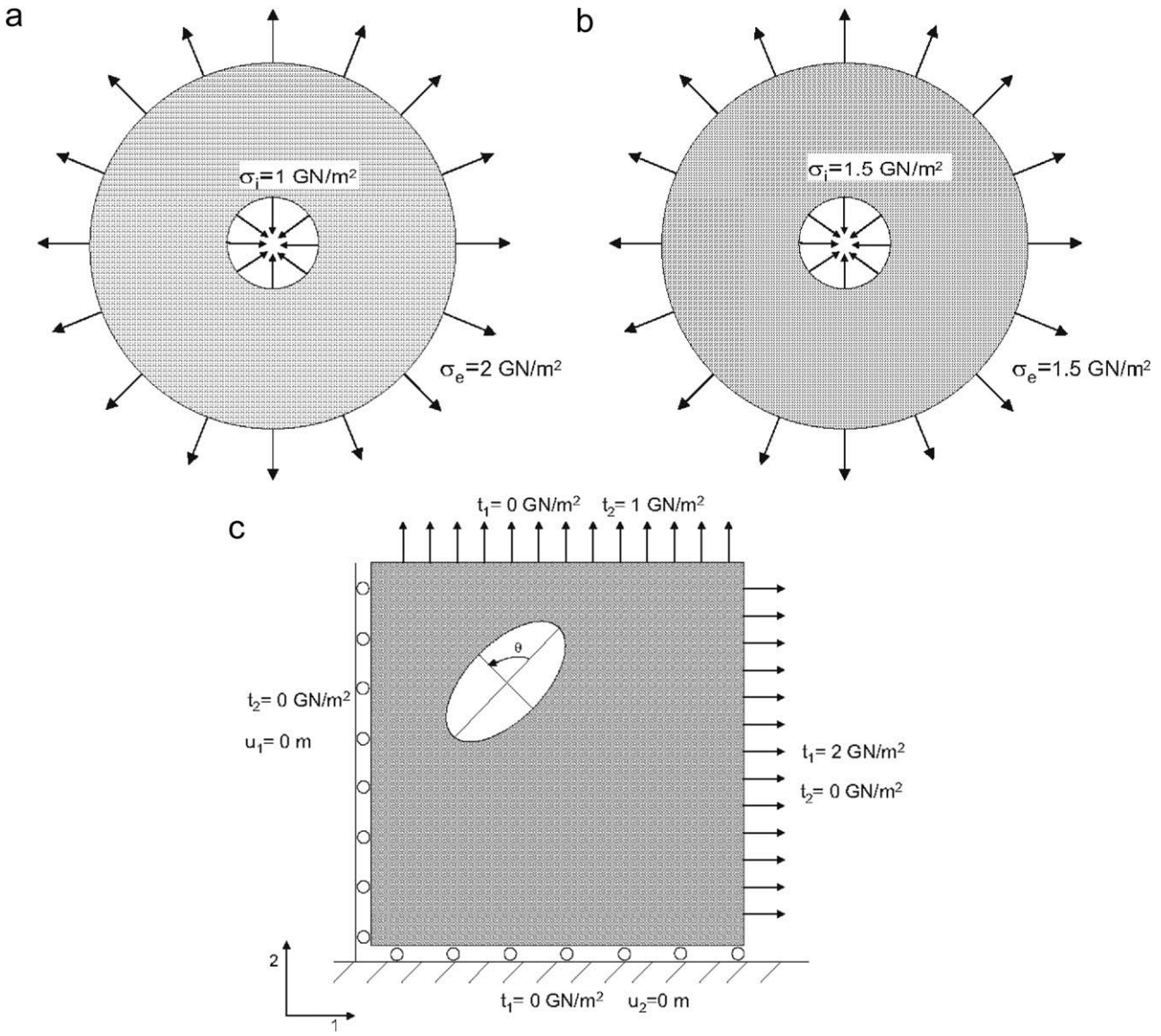

Fig. 1. The geometry and loading conditions for the Cauchy problems considered in Examples (a) 1, (b) 2, and (c) 3.

5.2. Initial guess

An arbitrary vector valued function $\mathbf{t}^{(0)} \in (H^{1/2}(\Gamma_1) \times H^{1/2}(\Gamma_1))^*$ may be specified as an initial guess for the traction vector on Γ_1, but in order to improve the rate of convergence of the iterative procedure we have chosen a vector valued function which ensures the continuity of the traction vector at the endpoints of Γ_1 and which is also linear with respect to the angular polar coordinate Θ. For Example 2, this initial guess is given by

$$\mathbf{t}^{(0)}(\mathbf{x}) = \frac{\alpha_2 - \Theta(\mathbf{x})}{\alpha_2 - \alpha_1}\mathbf{t}^{(0)}(\mathbf{x}_1) + \frac{\Theta(\mathbf{x}) - \alpha_1}{\alpha_2 - \alpha_1}\mathbf{t}^{(0)}(\mathbf{x}_2), \tag{24}$$

where $\alpha_i = \Theta(\mathbf{x}_i)$ for $i = 1, 2$, $\mathbf{x}_1$ and $\mathbf{x}_2$ are the endpoints of Γ_1, and the choice of $\alpha_1 = \pi/4$ and $\alpha_2 = 3\pi/4$ also ensures that the initial guess is not too close to the exact values $\mathbf{t}^{(\mathrm{an})}(\mathbf{x})$.

In the case of the other examples investigated, we cannot use the procedure described above and, therefore, the initial guess has been chosen as

$$\mathbf{t}^{(0)}(\mathbf{x}) = 0 \tag{25}$$

for Example 1 and

$$t_1^{(0)}(\mathbf{x}) = 2.0, \quad t_2^{(0)}(\mathbf{x}) = -3.0 \tag{26}$$

for Example 3.

5.3. Convergence of the algorithm

In order to investigate the convergence of the algorithm, at every iteration we evaluate the accuracy errors

defined by

$$E_u = \|\mathbf{u}^{(k)} - \mathbf{u}^{(\mathrm{an})}\|_{L^2(\Gamma_1)\times L^2(\Gamma_1)},$$
$$E_t = \|\mathbf{t}^{(k)} - \mathbf{t}^{(\mathrm{an})}\|_{L^2(\Gamma_1)\times L^2(\Gamma_1)}, \quad (27)$$

where $\mathbf{u}^{(k)}$ and $\mathbf{t}^{(k)}$ are the displacement and the traction vectors on the boundary Γ_1 retrieved after k iterations, respectively, and each iteration consists of solving the two mixed well-posed problems (7) and (8).

When starting with the initial guess $\mathbf{t}^{(0)}$ given by Eqs. (25) and (24) for Examples 1 and 2, respectively, a sequence $\{\mathbf{u}^{(k)}\}_{k>0}$ of approximation functions for $\mathbf{u}|_{\Gamma_1}$ is obtained and, according to Kozlov et al. [26], this sequence converges to the exact solution. If we evaluate the errors E_u and E_t at every iteration, in the case of Example 1, then we note that both these errors keep decreasing with respect to increasing the number of iterations performed only for the finest BEM mesh, i.e. $N_e = 96$, see Fig. 2. On the contrary, if the coarser BEM discretisations are used, i.e. $N_e = 32, 48$, then the accuracy errors given by expression (27) attain a minimum value after a certain iteration number, k, after which they start increasing. However, the errors E_u and E_t corresponding to the Cauchy problem given by Example 2 have a decreasing tendency as k increases for all the BEM discretisations used, see Fig. 3. A possible explanation for the different behaviours of the

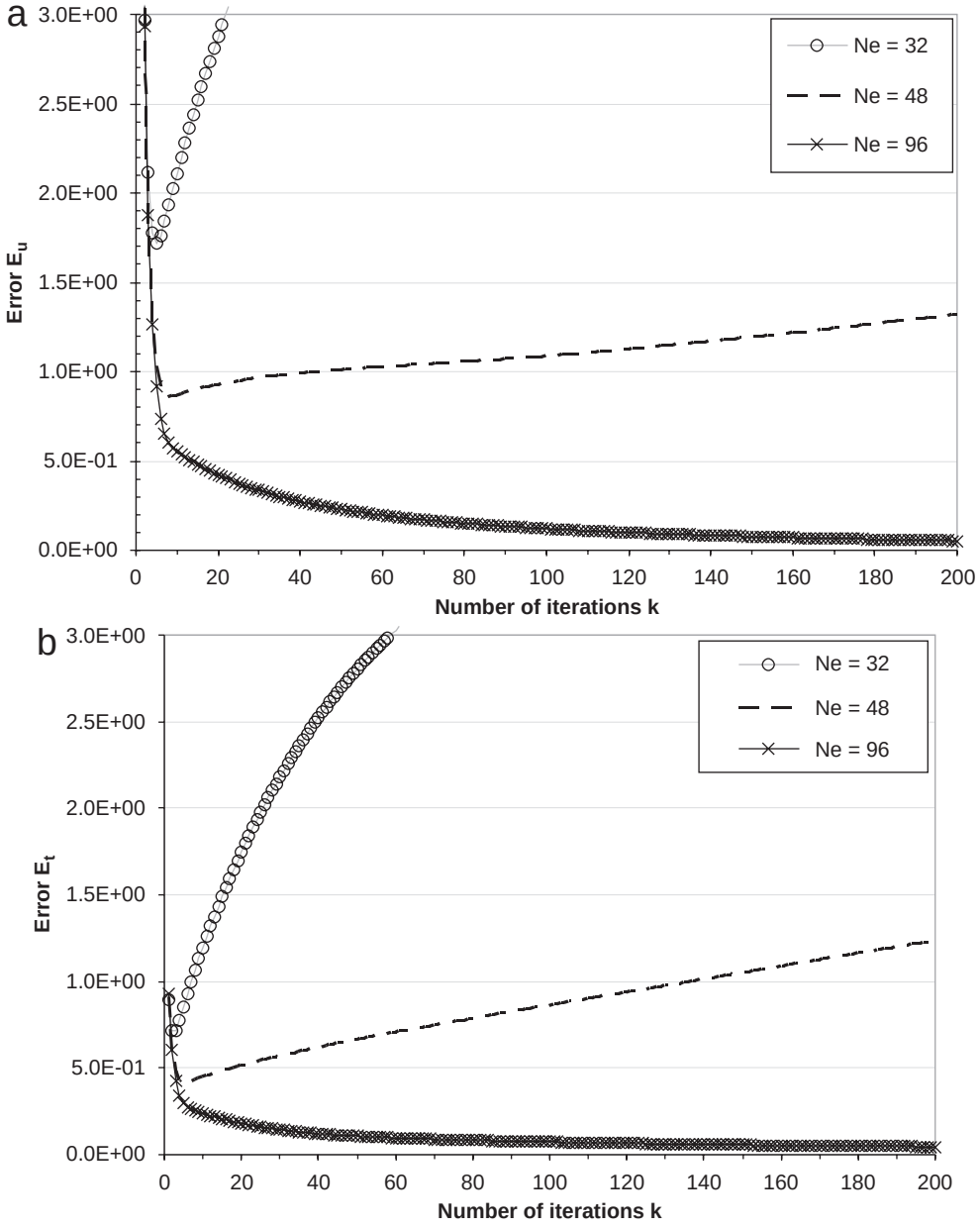

Fig. 2. The accuracy errors (a) E_u, and (b) E_t, as functions of the number of iterations, k, obtained using $N_e = 32$ ($-\circ-$), $N_e = 48$ ($- - -$) and $N_e = 96$ ($-\times-$) isoparametric quadratic boundary elements and exact Cauchy input data on the boundary Γ_2, for the Cauchy problem considered in Example 1.

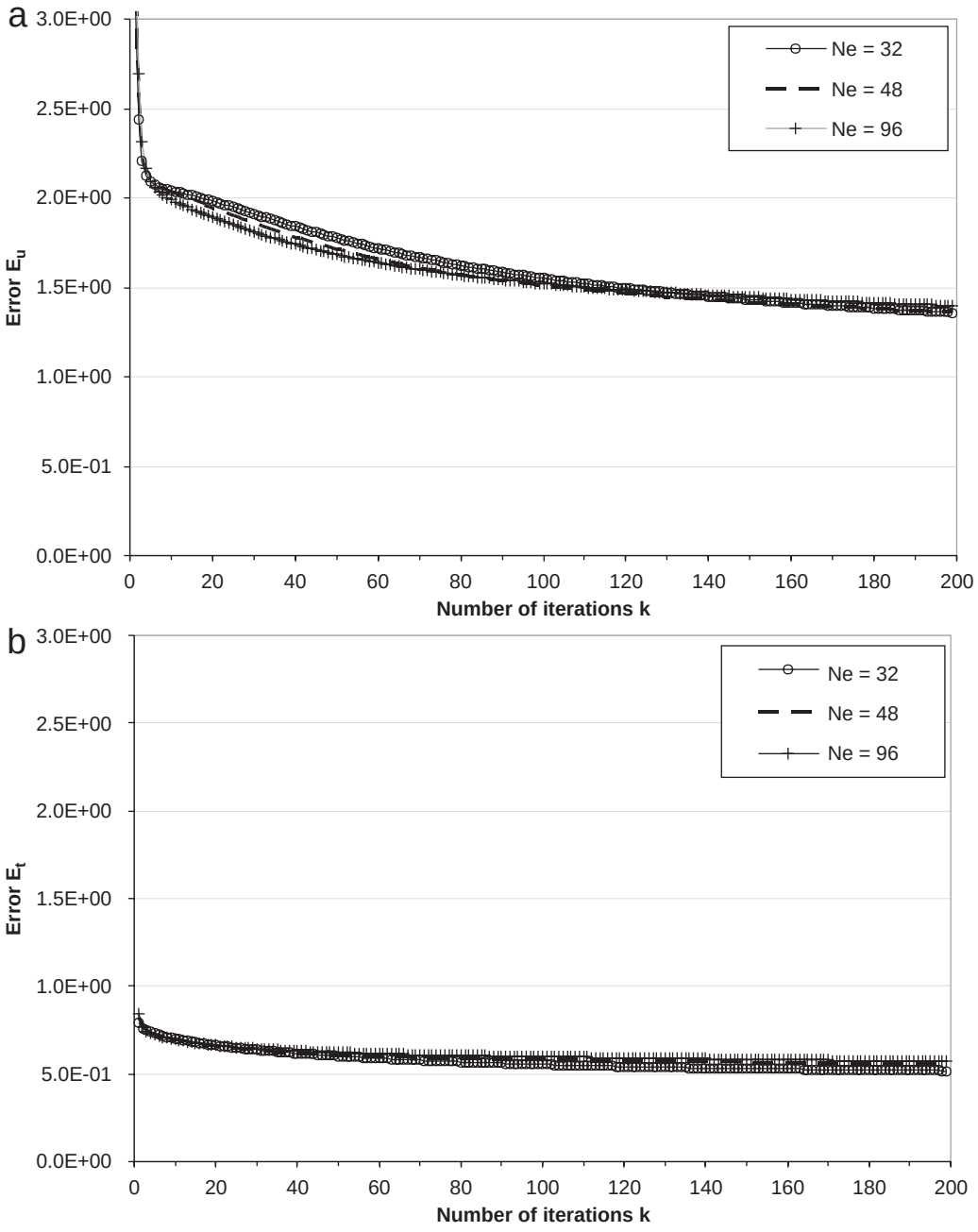

Fig. 3. The accuracy errors (a) E_u, and (b) E_t, as functions of the number of iterations, k, obtained using $N_e = 32$ $(-\circ-)$, $N_e = 48$ $(- - -)$ and $N_e = 96$ $(-+-)$ isoparametric quadratic boundary elements and exact Cauchy input data on the boundary Γ_2, for the Cauchy problem considered in Example 2.

accuracy errors E_u and E_t for Examples 1 and 2 is represented by the type of initial guess used for each of the Cauchy problems analysed. More precisely, the initial guess corresponding to Example 2 ensures the continuity of the traction vector at the endpoints of the under-specified boundary Γ_1, whereas the initial guess for the Example 1 is the constant vector zero which contains no information about the unknowns on Γ_1, see Eqs. (24) and (25), respectively.

We note that the algorithm proposed by Kozlov et al. [26] is convergent as we increase the number of boundary elements, as can be seen in Figs. 4 and 5 which represent the evolution of the numerical solutions for the x_1-component of the displacement and the x_2-component of the traction for the Cauchy problems associated with Examples 1 and 2, respectively, for $N_e \in \{32, 48, 96\}$. From Figs. 4 and 5 it can be seen that the numerical solutions for the displacement $u_1|_{\Gamma_1}$ and the traction $t_2|_{\Gamma_1}$ are more accurate for the Cauchy problem given by Example 1 than for the Cauchy problem corresponding to Example 2. The reason for this is that $\overline{\Gamma}_1 \cap \overline{\Gamma}_2 = \emptyset$ in the case of Example 1, whilst $\overline{\Gamma}_1 \cap \overline{\Gamma}_2 \neq \emptyset$ in the case of Example 2, i.e. there exist

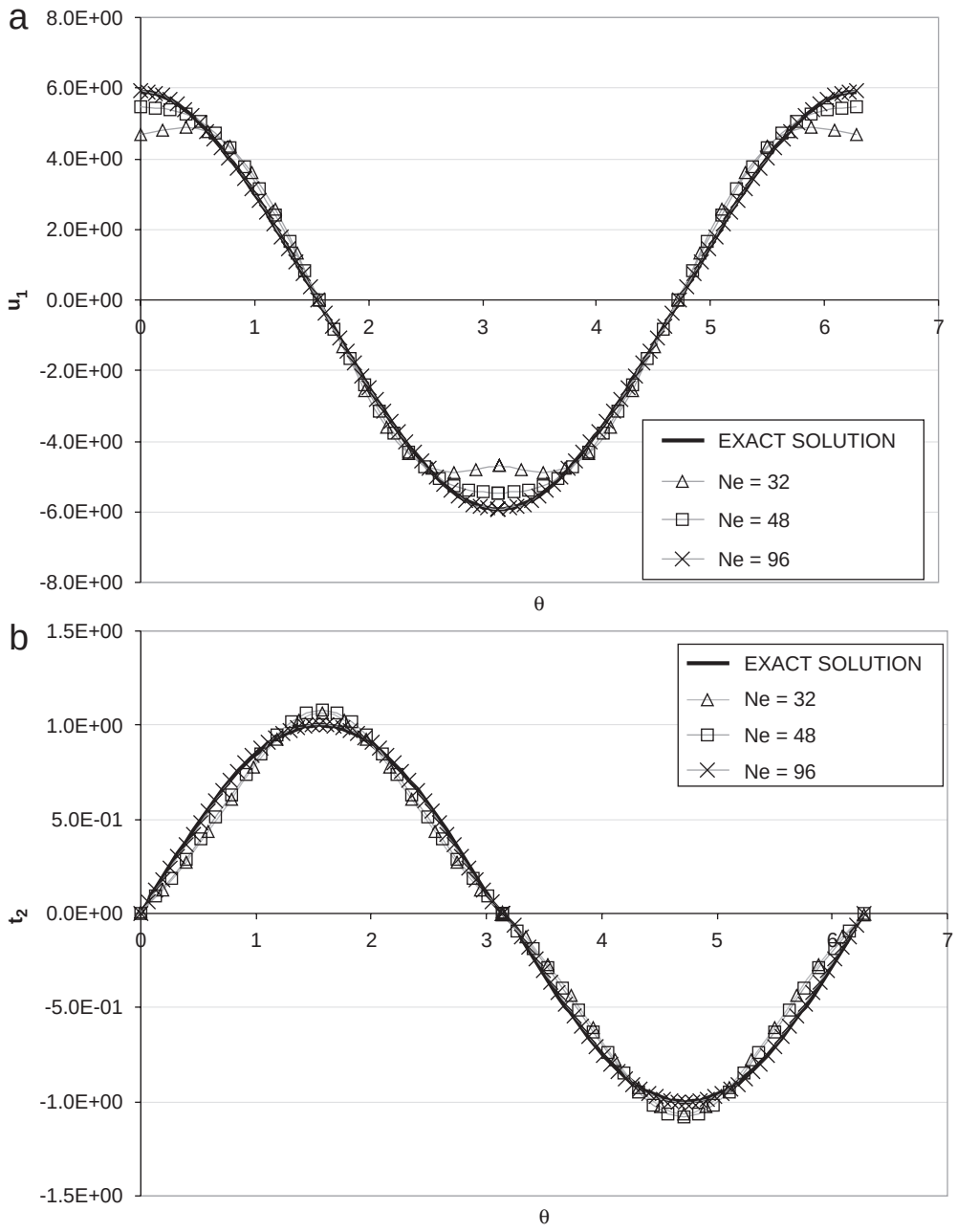

Fig. 4. (a) The exact $u_1^{(an)}$ (—) and the numerical $u_1^{(num)}$ displacements, and (b) the exact $t_2^{(an)}$ (—) and the numerical $t_2^{(num)}$ tractions, on the under-specified boundary Γ_1, obtained using $N_e = 32$ ($-\triangle-$), $N_e = 48$ ($-\square-$) and $N_e = 96$ ($-\times-$) isoparametric quadratic boundary elements, exact Cauchy input data on the boundary Γ_2 and $k = 200$ iterations, for the Cauchy problem considered in Example 1.

two points where the isoparametric quadratic BEM changes to mixed boundary conditions. It is well known, see e.g. Fichera [32] and Schiavone [33], that the gradient of the displacement **u** possesses singularities at the points where the data changes from displacement boundary conditions to traction boundary conditions, even if the displacement and the traction data are of class $\mathscr{C}^{\infty}$. Consequently, the classical solution for the displacement **u** cannot be smooth, although its smoothness can be improved if the displacement and the traction data are required to satisfy an increasing number (increasing with smoothness) of additional conditions, see also Wendland et al. [34]. Nevertheless, in the numerical implementation one may use weighted functions at each iteration of the algorithm in order to cancel the singularity, see Johansson [35], but this is deferred to future work.

5.4. Stopping criterion

Once the convergence with respect to increasing the number of boundary elements N_e of the numerical solution has been established, we investigate the stability of the

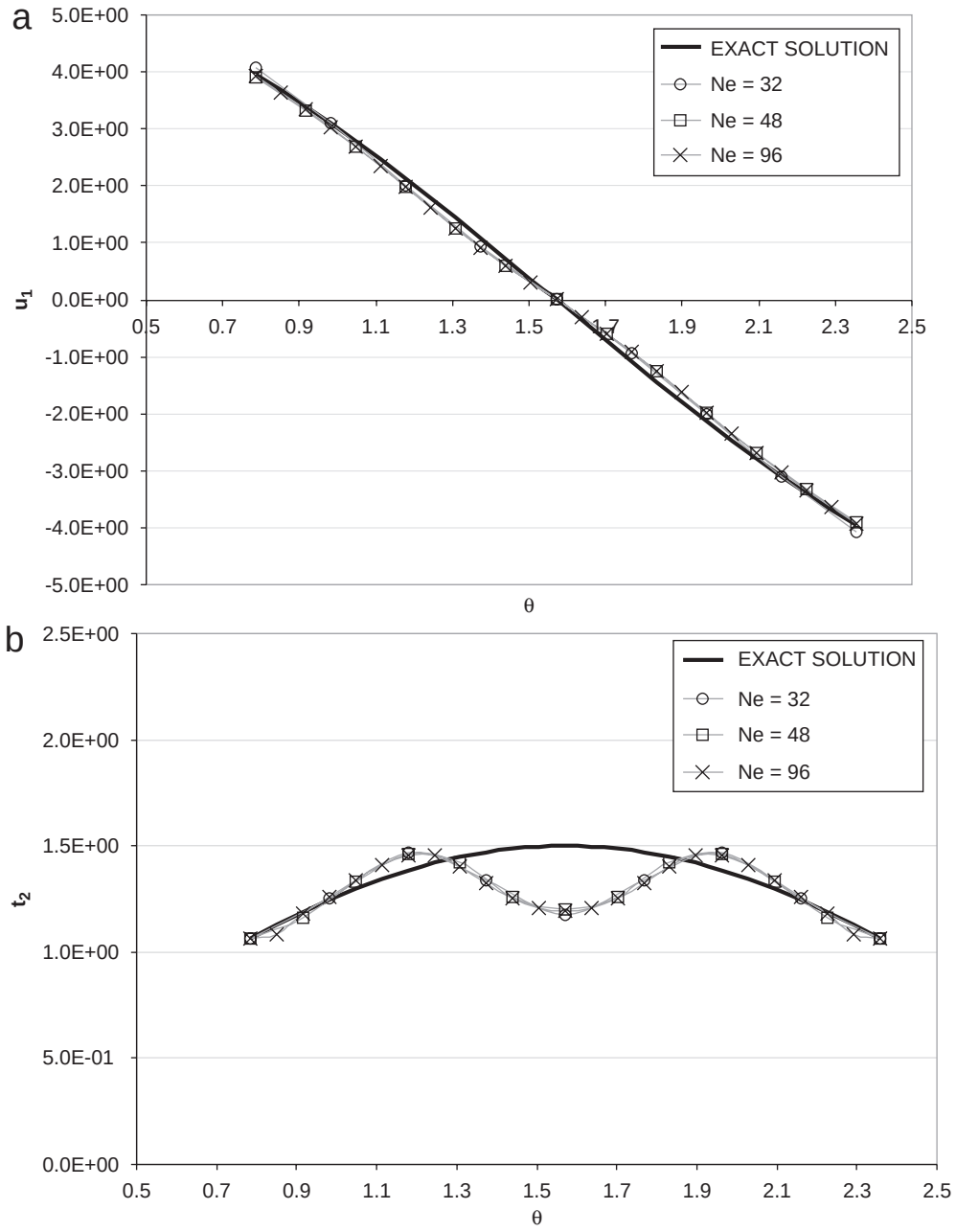

Fig. 5. (a) The exact $u_1^{(an)}$ (—) and the numerical $u_1^{(num)}$ displacements, and (b) the exact $t_2^{(an)}$ (—) and the numerical $t_2^{(num)}$ tractions, on the under-specified boundary Γ_1, obtained using $N_e = 32$ ($-\triangle-$), $N_e = 48$ ($-\square-$) and $N_e = 96$ ($-\times-$) isoparametric quadratic boundary elements, exact Cauchy input data on the boundary Γ_2 and $k = 200$ iterations, for the Cauchy problem considered in Example 2.

numerical solution for Example 3. To do so, we perturb the initial boundary displacements $\widetilde{u}_i|_{\Gamma_2}$, $i = 1, 2$, and/or tractions $\widetilde{t}_i|_{\Gamma_2}$, $i = 1, 2$, according to the following equations, $\widetilde{u}_i^{\varepsilon}|_{\Gamma_2} = \widetilde{u}_i|_{\Gamma_2} + \delta\widetilde{u}_i$, $i = 1, 2$, and $\widetilde{t}_i^{\varepsilon}|_{\Gamma_2} = \widetilde{t}_i|_{\Gamma_2} + \delta\widetilde{t}_i$, $i = 1, 2$, respectively. Here $\delta\widetilde{u}_i$, $i = 1, 2$, and $\delta\widetilde{t}_i$, $i = 1, 2$, are Gaussian random variables with mean zero and standard deviation $\sigma_i = \max_{\Gamma_2}|\widetilde{u}_i| \times (p/100)$, $i = 1, 2$, and $\sigma_i = \max_{\Gamma_2}|\widetilde{t}_i| \times (p/100)$, $i = 1, 2$, respectively, and p is the percentage of noise added into the input data $\widetilde{u}_i|_{\Gamma_2}$, $i = 1, 2$, or $\widetilde{t}_i|_{\Gamma_2}$, $i = 1, 2$. In Figs. 6(a) and (b) we present the accuracy error E_u corresponding to Example 3 for various levels of noise, namely $p \in \{1, 3, 5\}$, added into the Cauchy displacement and traction data, respectively. It can be seen from these figures that the error E_u decreases up to a certain number of iterations, after which it starts increasing. If the process is continued beyond this point then the numerical solutions lose their smoothness and become highly oscillatory and unbounded. Therefore, a regularising stopping criterion must be used in order to cease the iterative process at the point where the errors in the numerical solutions start increasing. Although not presented herein, it is reported that the accuracy error E_t has a similar behaviour.

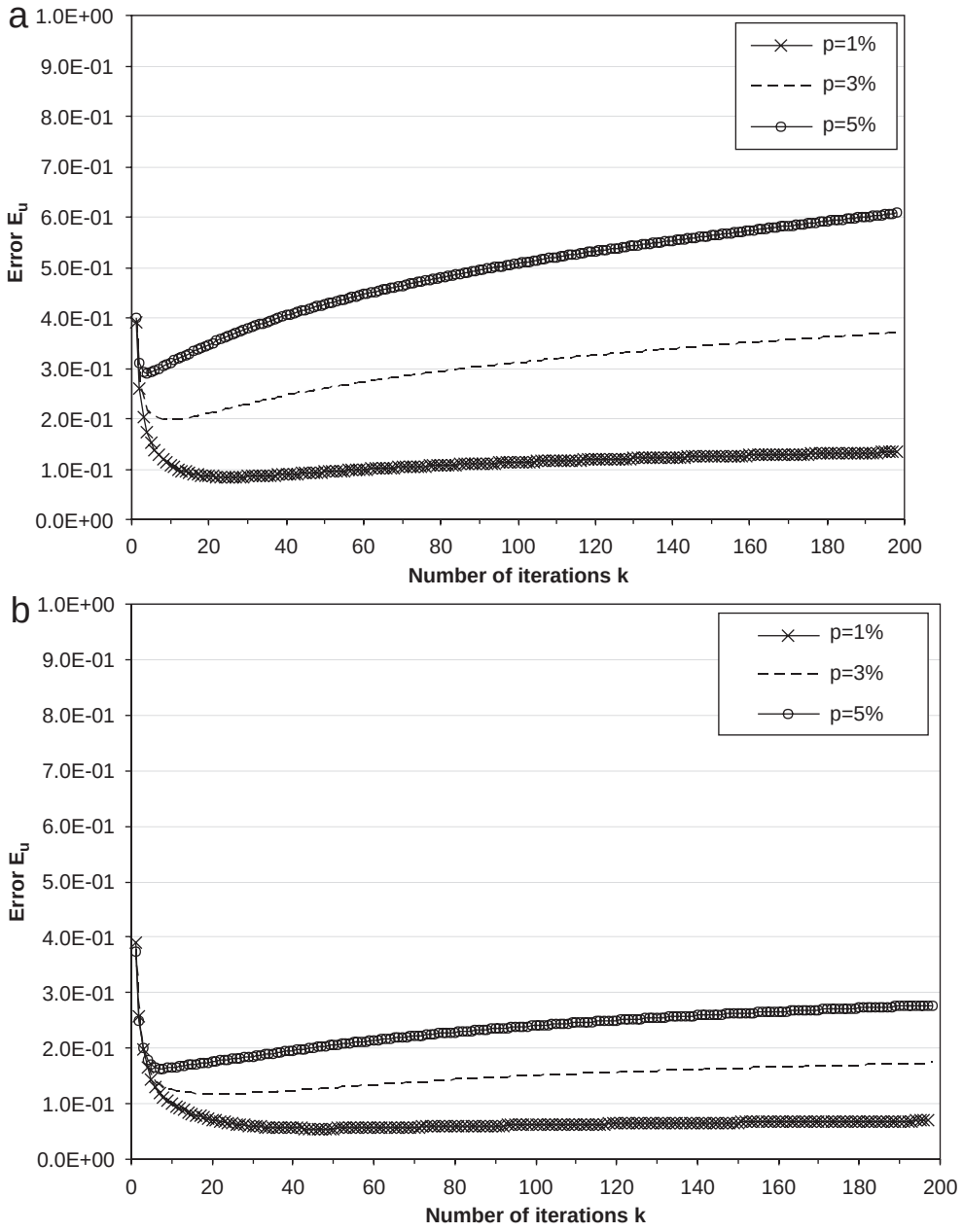

Fig. 6. The accuracy error E_u as a function of the number of iterations, k, obtained using several amounts of noise added into the input data (a) $\mathbf{u}|_{\Gamma_2}$, and (b) $\mathbf{t}|_{\Gamma_2}$, namely $p = 1\%$ $(- \times -)$, $p = 3\%$ $(- - -)$ and $p = 5\%$ $(- \circ -)$, for the Cauchy problem considered in Example 3.

If we evaluate the Euclidean norm of the vector $\mathbf{CX} - \mathbf{F}$, then this should tend to zero as $\mathbf{X}$ tends to the exact solution. Hence after each iteration we evaluate the error

$$E = \|\mathbf{CX}^{(k)} - \mathbf{F}\|_2, \tag{28}$$

where $\mathbf{X}^{(k)}$ is the vector obtained from the values of the displacement and the traction vectors on the boundary Γ_1 retrieved after k iterations. The error E includes information on both the displacement and the traction vectors and it is expected to provide an appropriate stopping criterion. If we investigate the error E obtained at every iteration for the example considered for various levels of noise added into the input data $\widetilde{\mathbf{u}}|_{\Gamma_2}$ and $\widetilde{\mathbf{t}}|_{\Gamma_2}$, we obtain the curves graphically represented in Figs. 7(a) and (b), respectively.

Regularisation is necessary when solving ill-posed inverse problems such as the Cauchy problem in anisotropic linear elasticity. By adding regularisation, we are able to damp out the contributions from data and rounding errors, and maintain the solution norm to be of reasonable size. It should be mentioned that in the case of the alternating iterative algorithm described in Section 3, the regularisation parameter is given by the number of iterations performed, k. If too much regularisation, i.e. the

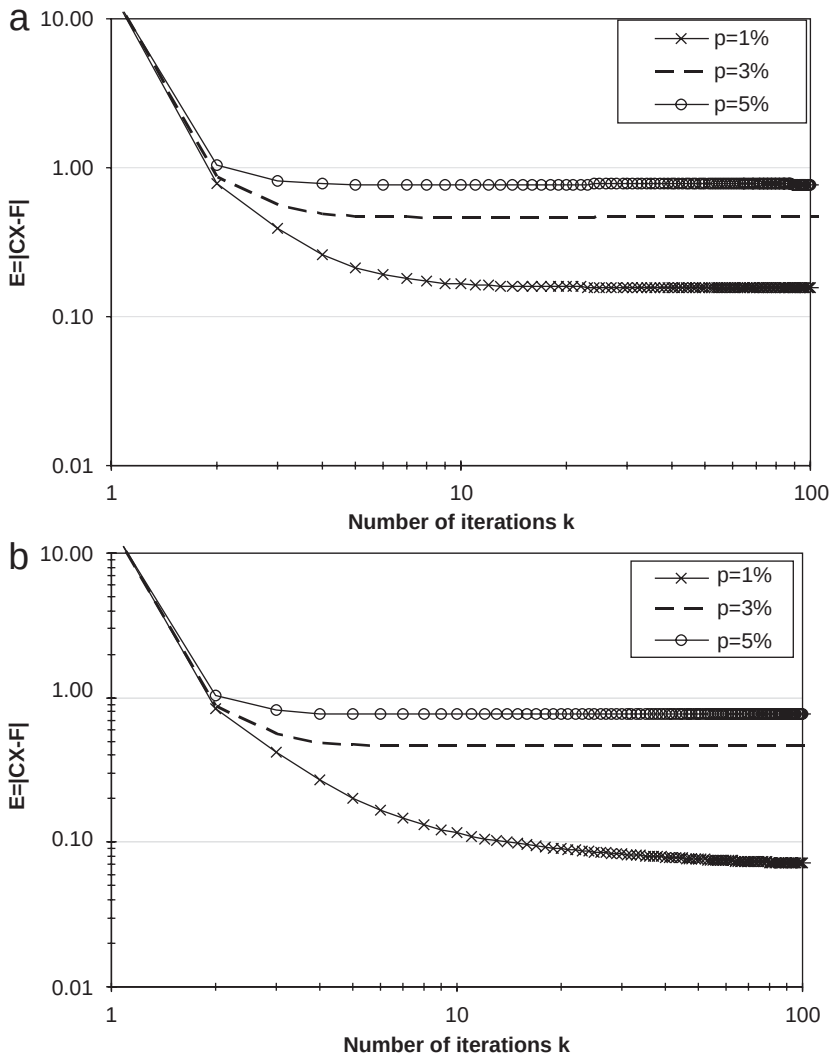

Fig. 7. The convergence error $E = \|\mathbf{CX} - \mathbf{F}\|_2$ as a function of the number of iterations, k, obtained using several amounts of noise added into the input data (a) $\mathbf{u}|_{\Gamma_2}$, and (b) $\mathbf{t}|_{\Gamma_2}$, namely $p = 1\%$ $(- \times -)$, $p = 3\%$ $(- - -)$ and $p = 5\%$ $(- \circ -)$, for the Cauchy problem considered in Example 3.

number of iterations performed, k, is too small, is imposed on the solution, it will not fit the data $\mathbf{F}$ and the residual norm $\|\mathbf{CX}^{(k)} - \mathbf{F}\|_2$ will be too large. If too little regularisation is imposed on the solution, i.e. the number of iterations performed, k, is too large, then the fit will be good, but the solution will be dominated by the contributions from the data errors and, consequently, the solution norm $\|\mathbf{X}^{(k)}\|_2$ will be too large. Therefore, the iterative process is stopped at the iteration number, k_{opt}, corresponding to the corner of the curves represented in Figs. 7(a) and (b), where the error E starts to become constant. Indeed, from Figs. 6 and 7 it can be seen that the proposed stopping criterion is very efficient in locating the point where the errors in the numerical solution increase and the iterative process should be terminated, although more rigorous stopping criteria, such as the discrepancy principle [36] or the generalised cross-validation [37], could have been used.

5.5. Stability of the algorithm

Based on the stopping criterion described in the previous section, the numerical results for the displacement u_2 and the traction t_1 on the under-specified boundary Γ_1, obtained using various levels of noise added into $\mathbf{u}|_{\Gamma_2}$ and $\mathbf{t}|_{\Gamma_2}$, for Example 3 are presented in Figs. 8 and 9, respectively. From these figures it can be seen that the numerical solution is a stable approximation to the exact solution, free of unbounded and rapid oscillations. Furthermore, by comparing Figs. 6, 8 and 9, it can be noticed that the numerical results are more sensitive to noise added into the displacement Cauchy data than to noise added into the traction Cauchy data. Although not presented, it is reported that similar results have been obtained for the displacement and traction vectors on the under-specified boundary Γ_1 when applying the stopping criterion described in the previous section to Examples 1

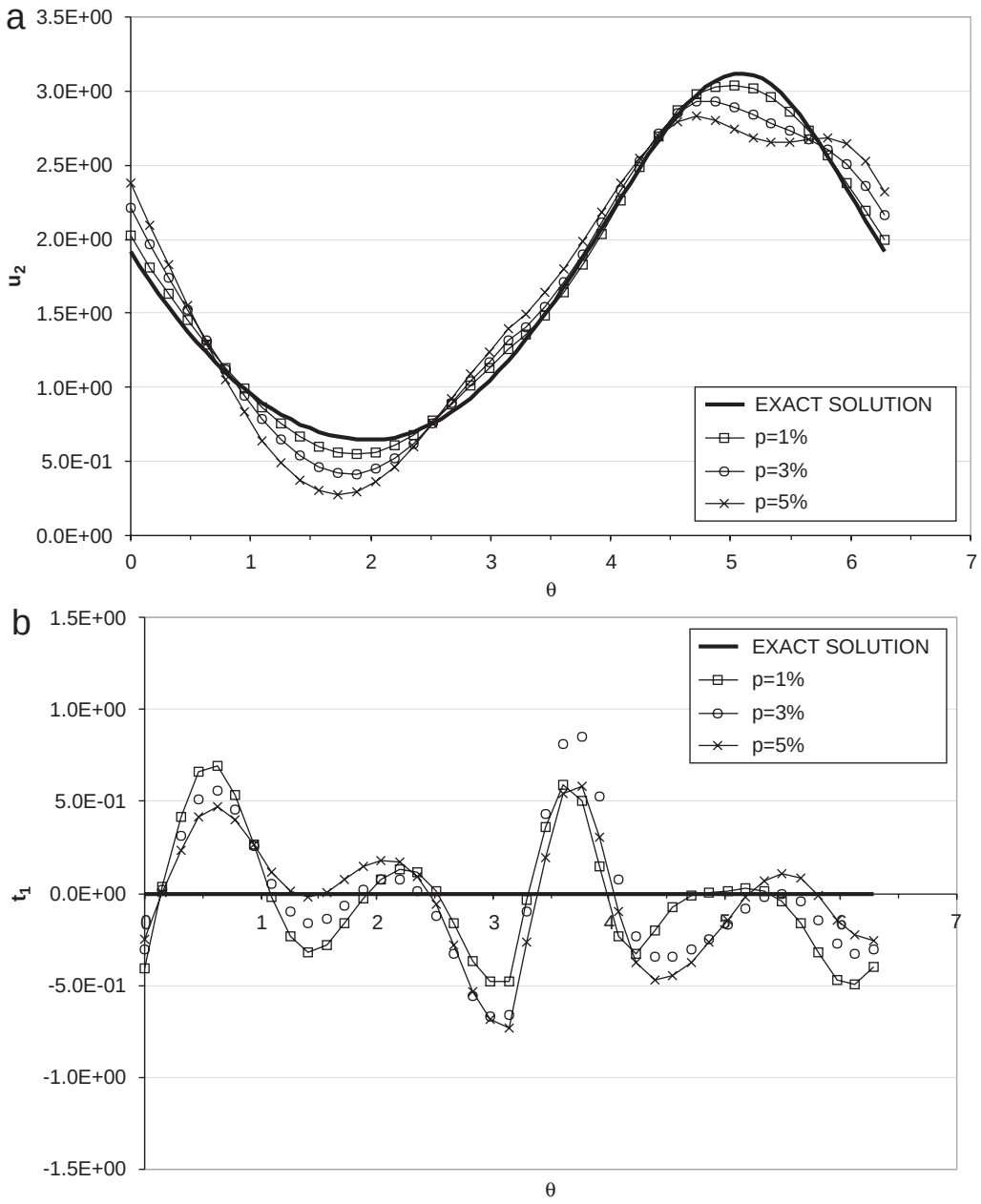

Fig. 8. (a) The exact $u_2^{(an)}$ (—) and the numerical $u_2^{(num)}$ displacements, and (b) the exact $t_1^{(an)}$(—) and the numerical $t_1^{(num)}$ tractions, on the under-specified boundary Γ_1, obtained using several amounts of noise added into the input data $\mathbf{u}|_{\Gamma_2}$, namely $p = 1\%$ $(-\square-)$, $p = 3\%$ $(-\circ-)$ and $p = 5\%$ $(-\times-)$, for the Cauchy problem considered in Example 3.

and 2. From the numerical results presented in this section it can be concluded that the stopping criterion developed in Section 5.4 has a regularising effect and the numerical solution obtained by the iterative BEM described in this study is convergent and stable with respect to increasing the mesh size discretisation and decreasing the level of noise, respectively.

6. Conclusions

In this paper the Cauchy problem in two-dimensional anisotropic linear elasticity was investigated as an extension of a previous analysis of the Cauchy problem associated with two-dimensional isotropic linear elastic materials, see e.g. Marin et al. [13]. In order to deal with the instabilities of the solution of this ill-posed problem, an iterative BEM was employed which reduced the Cauchy problem to a sequence of well-posed mixed boundary value problems. A regularising stopping criterion, necessary for ceasing the iterations at the point where the accumulation of noise becomes dominant and the errors in predicting the exact solution increase, has also been presented. The numerical results obtained for various numbers of boundary elements and various levels of noise added into the

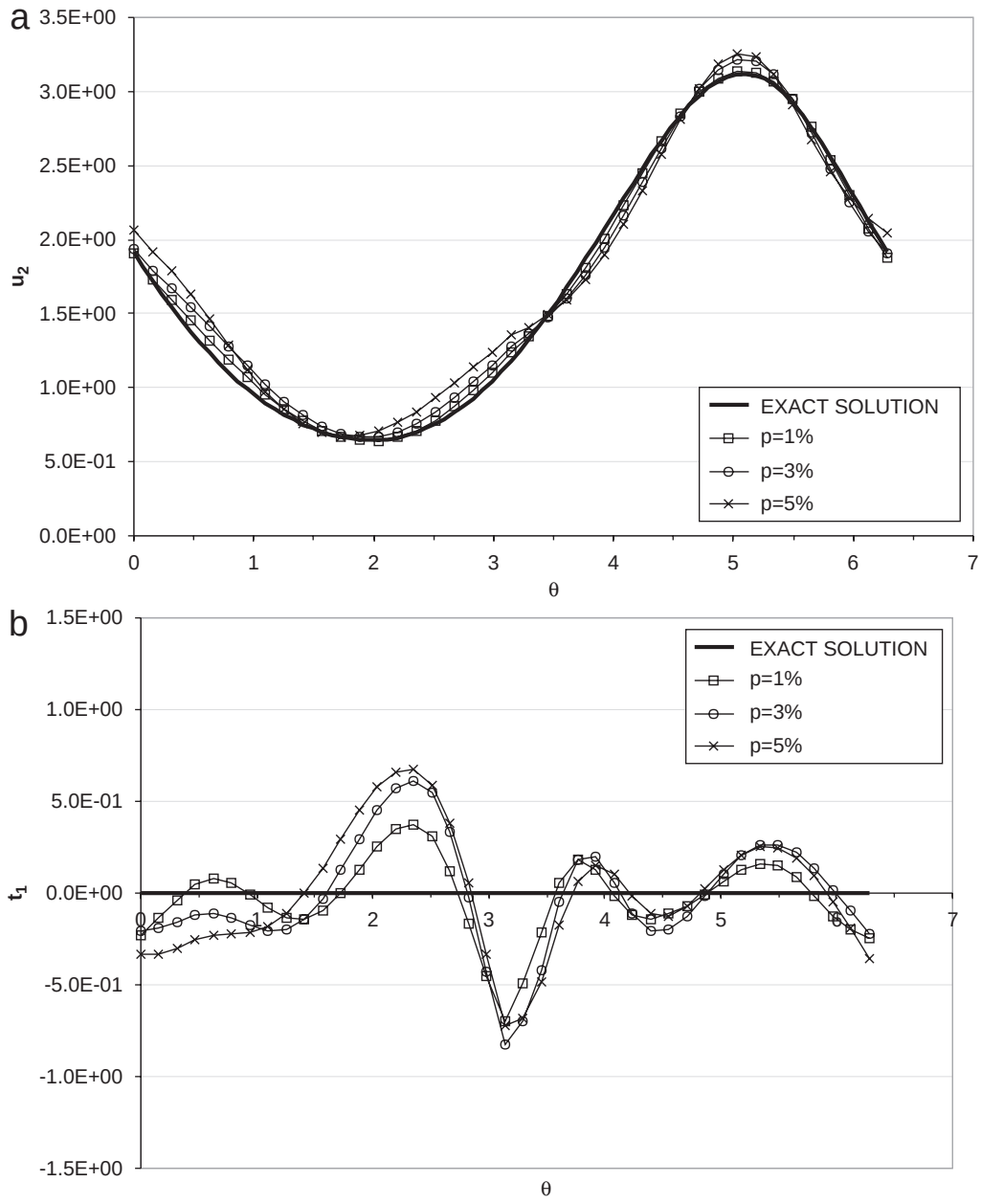

Fig. 9. (a) The exact $u_2^{(an)}$ (—) and the numerical $u_2^{(num)}$ displacements, and (b) the exact $t_1^{(an)}$ (—) and the numerical $t_1^{(num)}$ tractions, on the under-specified boundary Γ_1, obtained using several amounts of noise added into the input data $\mathbf{t}|_{\Gamma_2}$, namely $p = 1\%$ $(-\square-)$, $p = 3\%$ $(-\circ-)$ and $p = 5\%$ $(-\times-)$, for the Cauchy problem considered in Example 3.

input data were found to be in very good agreement with the exact solution. From the examples investigated in this study it can be concluded that the alternating iterative BEM produces a convergent, stable and consistent numerical solution with respect to refining the mesh size and decreasing the amount of noise.

Appendix A. Evaluation of the integration constants

When evaluating the integrals given by relations (18) and (19), we must take into account two distinct situations depending on whether the collocation point l belongs or does not to the element over which the integration is performed. The first situation, also called the *ordinary case*, presents no difficulty and can be evaluated numerically using a Gaussian quadrature. The Cauchy principal value (CPV) has meaning only in the later case which is known as the *singular case*. However, this situation needs some more attention.

On developing expression (18) for the integration constants $h_{ij}^m(l,k)$, we obtain the following integral:

$$h_{ij}^m(l,k) = 2\,\mathrm{Re}\left[\int_{-1}^{1}\sum_{s=1}^{2}\frac{q_{js}A_{is}}{z_s(\xi)-y_s^l}(\mu_s n_1 - n_2)\phi_m J^k\,\mathrm{d}\xi\right], \tag{A.1}$$

which requires the evaluation of the complex integral

$$I_s = \int_{-1}^{1} \frac{\mu_s n_1 - n_2}{z_s(\xi) - y_s^l} \phi_m J^k \, \mathrm{d}\xi. \tag{A.2}$$

In the singular case, the integral I_s can be split into a regular integral $\bar{I}_s$ and an integral in the CPV sense as follows:

$$I_s = \bar{I}_s + \int_{-1}^{1} \frac{\phi_m}{\xi - \xi_l} \, \mathrm{d}\xi, \tag{A.3}$$

where ξ_l is the natural coordinate of the collocation point. The CPV integral is solved taking into account the fact that the two infinite terms occurring for $\xi_l = 1$ and -1 cancel out when the evaluation is performed over two adjacent elements

$$\int_{-1}^{1} \frac{\phi_m}{\xi - \xi_l} \, \mathrm{d}\xi = \int_{-1}^{1} \frac{a\xi^2 + b\xi + c}{\xi - \xi_l} \, \mathrm{d}\xi = a\xi_l + 2b + \phi_m(\xi_l) \ln \frac{1 - \xi_l}{1 + \xi_l}. \tag{A.4}$$

For the integration constants $g_{ij}^m(l,k)$, relation (19) may be recast as

$$g_{ij}^m(l,k) = 2\,\mathrm{Re}\left[\int_{-1}^{1} \sum_{s=1}^{2} p_{js} A_{is} \ln[z_s(\xi) - y_s^l] \phi_m J^k \, \mathrm{d}\xi \right], \tag{A.5}$$

and hence another complex expression I_s must be evaluated, namely

$$I_s = \int_{-1}^{1} \ln[z_s(\xi) - y_s^l] \phi_m J^k \, \mathrm{d}\xi. \tag{A.6}$$

In the singular case, if $l \in k$ then the integral I_s becomes improper but after some manipulation it can be calculated using the following integral:

$$\int_0^1 \ln\left(\frac{1}{\eta}\right) f(\eta) \, \mathrm{d}\eta. \tag{A.7}$$

A specific Gaussian quadrature suitable for computing the integral (A.7) is further employed, namely

$$\int_0^1 \ln\left(\frac{1}{\eta}\right) f(\eta) \, \mathrm{d}\eta \approx \sum_{k=1}^{n} w_k' f(\eta_k'), \tag{A.8}$$

where w_k' is the weight coefficient and η_k' is the coordinate for the quadrature, see e.g. Brebbia and Dominguez [30].

References

[1] Knops RJ, Payne LE. Uniqueness theorems in linear elasticity. Berlin: Springer; 1972.

[2] Hadamard J. Lectures on Cauchy problem in linear partial differential equations. London: Oxford University Press; 1923.

[3] Beck JV, Blackwell B, St Clair CR. Inverse heat conduction: ill-posed problems. New York: Wiley-Interscience; 1985.

[4] Ikehata M. How to draw a picture of an unknown inclusion from boundary measurements. Two mathematical inversion algorithms. J Inverse Ill-Posed Probl 1999;7:255–71.

[5] Colton D, Kress R. Inverse acoustic and electromagnetic scattering. Berlin: Springer; 1992.

[6] Kubo S. Inverse problems related to the mechanics and fracture of solids and structures. JSME Int J 1988;31:157–66.

[7] Chen JT, Chen KH. Analytical study and numerical experiments for Laplace equation with overspecified boundary conditions. Appl Math Modelling 1998;22:703–25.

[8] Maniatty A, Zabaras N, Stelson K. Finite element analysis of some elasticity problems. J Eng Mech Div ASCE 1989;115:1302–16.

[9] Zabaras N, Morellas V, Schnur D. Spatially regularized solution of inverse elasticity problems using the BEM. Commun Appl Numer Methods 1989;5:547–53.

[10] Schnur D, Zabaras N. Finite element solution of two-dimensional elastic problems using spatial smoothing. Int J Numer Methods Eng 1990;30:57–75.

[11] Yeih WC, Koya T, Mura T. An inverse problem in elasticity with partially overspecified boundary conditions. I. Theoretical approach. Trans ASME J Appl Mech 1993;60:595–600.

[12] Koya T, Yeih WC, Mura T. An inverse problem in elasticity with partially overspecified boundary conditions. II. Numerical details. Trans ASME J Appl Mech 1993;60:601–6.

[13] Marin L, Elliott L, Ingham DB, Lesnic D. Boundary element method for the Cauchy problem in linear elasticity. Eng Anal Boundary Elem 2001;25:783–93.

[14] Marin L, Elliott L, Ingham DB, Lesnic D. An alternating boundary element algorithm for a singular Cauchy problem in linear elasticity. Comput Mech 2002;28:479–88.

[15] Huang CH, Shih WY. A boundary element based solution of an inverse elasticity problem by conjugate gradient and regularisation method. In: Proceedings of the seventh international offshore polar engineering conference, Honolulu, USA; 1997. p. 383–95.

[16] Marin L, Háo DN, Lesnic D. Conjugate gradient—boundary element method for the Cauchy problem in elasticity. Q J Mech Appl Math 2002;55:227–47.

[17] Marin L, Lesnic D. Regularized boundary element solution for an inverse boundary value problem in linear elasticity. Commun Numer Methods Eng 2002;18:817–25.

[18] Marin L, Lesnic D. Boundary element solution for the Cauchy problem in linear elasticity using singular value decomposition. Comput Methods Appl Mech Eng 2002;191:3257–70.

[19] Marin L, Elliott L, Ingham DB, Lesnic D. Boundary element regularisation methods for solving the Cauchy problem in linear elasticity. Inverse Probl Eng 2002;10:335–57.

[20] Marin L, Lesnic D. The method of fundamental solutions for the Cauchy problem in two-dimensional linear elasticity. Int J Solids Struct 2004;41:3425–38.

[21] Marin L, Lesnic D. Boundary element—Landweber method for the Cauchy problem in linear elasticity. IMA J Appl Math 2005; 70:323–40.

[22] Lavrent'ev MM. Some ill-posed problems of mathematical physics. Novosibirsk: Izdet. Sibirsk. Otdel. Akad. Nauk SSSR; 1962 [in Russian].

[23] Tikhonov AN, Arsenin VY. Methods for solving ill-posed problems. Moscow: Nauka; 1986.

[24] Bakushinsky A, Goncharsky A. Ill-posed problems: theory and applications. Dordrecht: Kluwer Academic Publishers; 1994.

[25] Morozov VA. Methods for the solution of ill-posed problems. Moscow: Nauka; 1986.

[26] Kozlov VA, Maz'ya VG, Fomin AF. An iterative method for solving the Cauchy problem for elliptic equations. USSR Comput Math Math Phys 1991;31:45–52.

[27] Lekhnitskii SG. Theory of elasticity of an anisotropic body. Moscow: Mir Publishers; 1981.

[28] Lions JL, Magenes E. Non-homogeneous boundary value problems and their applications. New York, Heidelberg: Springer; 1972.

[29] Sollero P. Fracture mechanics analysis of anisotropic laminates by the boundary element method. PhD Thesis, Wessex Institute of Technology; 1994.

[30] Brebbia CA, Dominguez J. Boundary elements: an introductory course. London: McGraw-Hill; 1992.
[31] París F, Cañas J. Boundary element method. Fundamentals and applications. London: Oxford University Press; 1997.
[32] Fichera G. Sul problema della derivata obliqua e sul problema misto per l'equazione di Laplace. Boll Un Mat Ital 1952;7:367–77.
[33] Schiavone P. Mixed problem in the theory of elastic plates with transverse shear deformation. Q J Mech Appl Math 1997;50: 239–49.
[34] Wendland WL, Stephan E, Hsiao GC. On the integral equation method for the plane mixed boundary value problem for the Laplacian. Math Methods Appl Sci 1979;1:265–321.
[35] Johansson T. An iterative procedure for solving a Cauchy problem for second order elliptic equations. Math Nachr 2004;272:46–54.
[36] Morozov VA. On the solution of functional equations by the method of regularisation. Sov Math Dokl 1966;7:414–7.
[37] Wahba G. Practical approximate solutions to linear operator equations when the data are noisy. SIAM J Numer Anal 1977; 14:651–67.